Phase diagram of layered quasi-one-dimensional conductors in a magnetic field

A. G. Lebed'

L. D. Landau Institute of Theoretical Physics, Academy of Sciences of the USSR
(Submitted 1 April 1985)
Zh. Eksp. Teor. Fiz. **89**, 1034–1049 (September 1985)

A study is made of the phase diagram of a two-dimensional anisotropic conductor in a magnetic field. It is shown that the problem of finding the free energy reduces to a certain effective Peierls problem, while the phase diagram consists of a series of excitonic subphases. The stability curve $T(H)$ for a layered quasi-one-dimensional conductor is determined, and it is found that the transition temperature and other physical quantities can undergo "rapid" and "slow" oscillations with periods in the inverse field of $2\pi e\hbar/cS$ and $\pi e\hbar t_b/cSt_c$, where t_b and t_c are the tunneling integrals and S is the effective area of the "orbits." The results are compared with the experimentally observed oscillations of $(TMTSF)_2ClO_4$.

1. INTRODUCTION

A large body of experimental material has accumulated on the properties of the so-called Bechgaard salts—the compounds $(TMTSF)_2X$, where $S = ClO_4$, PF_6, AsF_6, etc. (see reviews[1,2]). These substances have been synthesized in the search for quasi-one-dimensional superconducting materials. In addition to superconductivity, Bechgaard salts exhibit a number of other interesting properties, many of which do not have familiar analogs. The latter include, first of all, the unusual behavior of these compounds in a magnetic field at low temperatures. These properties are most conveniently summarized by means of the phase diagram in (T,P,H) space; such diagrams have been obtained experimentally for $X = ClO_4$ and $X = PF_6$ (Fig. 1). The cross-hatched part of the surface for $H > H_0$ is found[3,4] to correspond to the phase boundary (in terms of the field) between the anisotropic metallic phase and field-induced magnetic semimetallic phases (MSPs).

The states on this diagram for $H > H_0$ are manifested in unexpected physical phenomena. The existence of semimetallic subphases was first detected on the basis of features in the magnetoresistance.[3,4] They were originally interpreted in terms of Shubnikov–de Haas oscillations. The atypical properties of these oscillations and the subsequent observation of jumps in the Hall voltage led to the idea[5,6] that there was actually a whole series of phase transitions to a magnetic state with a spin-density wave (SDW). We emphasize again that for $H < H_0$ there is an ordinary anisotropic metallic state with a high conductivity and that the observed transitions are undoubtedly induced by the field.

The layered nature of the compounds $(TMTSF)_2X$ will be essential to our understanding of the features of the phase diagram of these compounds. It has been shown[7] that layered metals in a magnetic field are unstable against the formation of a spin-density wave. We shall link the features of the properties of Bechgaard salts to just this instability.

Let us review the instability mechanism.[7] For quasiclassical electrons moving along open trajectories, the motion in real space is along the directions perpendicular to the openness. In a magnetic field their transverse motion is bounded. Moreover, they take on one-dimensional properties—the electrons and holes on opposite sides of the Fermi surface do not separate to infinity in the transverse direction. If there is an attraction between them (Coulomb interaction) they easily form pairs, giving rise to a spin or Peierls instability. Which of the two instabilities develops depends on the specific circumstances. In the substances under discussion at $P = 0$ it is the spin instability that occurs. The metallic state in Fig. 1 is the result of the destruction of the SDW phase by pressure. Consequently, near the threshold the mechanism described above will result in the restoration of the SDW state even in a weak field.

The goal of the present study is to carry out a more detailed analysis of the SDW or charge-density wave (CDW) instability in layered compounds and, in particular, to study the possible structure of the various subphases. The experimental material corresponds well to the model chosen below. With this in mind, let us begin with a brief discussion of certain features of the electronic spectrum of Bechgaard salts and the associated features of the phase diagram in the absence of a magnetic field. Next, in Sec. 3 the instability in a magnetic field will be demonstrated under quite general assumptions. Finally, in Secs. 4–6 the phase transition temperature and the phase diagram below the transition point will be studied in reference to the specific electronic spectrum of the compounds $(TMTSF)_2X$. In the Conclusion our results are compared with the experimental situation.

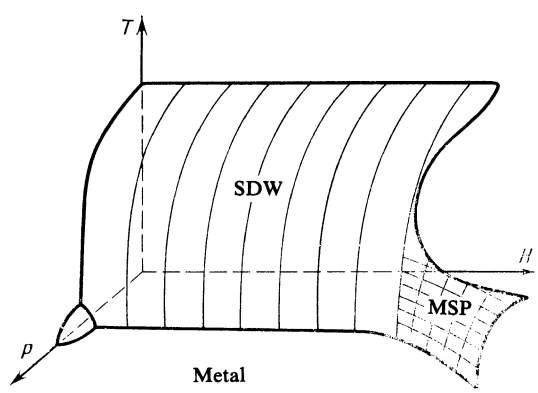

FIG. 1.

2. DEGENERATE ELECTRONIC SPECTRUM

It is customarily assumed (see, e.g., Ref. 1) that the extremely simple electronic spectrum

$$\varepsilon_{1,2}(p_\parallel, \mathbf{p}_\perp) = \pm v(p_\parallel \mp k_F) + 2t_b \cos(p_b b^*) + 2t_c \cos(p_c c^*), \quad (1)$$

which corresponds to the tight binding model in an orthorhombic lattice, gives a good description of the properties of Bechgaard salts (b^* and c^* are the axes of the resistivity tensor). The experimental estimates of the overlap integrals, $t_b/t_c \approx 10$–30, reflect the layered nature of these compounds. Consequently, in a first approximation the electronic spectrum can be assumed two-dimensional:

$$\varepsilon_{1,2}(p_\parallel, \mathbf{p}_\perp) = \pm v(p_\parallel \mp k_F) + 2t_b \cos(p_b b^*). \quad (1')$$

Electronic spectra (1) and (1′) have a number of features. For example, for the choice[8] of wave vector $\mathbf{Q}_0 = (2k_F, \pi/b^*, \pi/c^*)$ there is perfect nesting, i.e., an exact superposition of the right and left parts of the Fermi surface. This mechanism in and of itself could lead to the formation of an insulating SDW (CDW) state.[9] For some time this mechanism was assumed to be responsible for the formation of the SDW phase in the compounds under study. However, the first estimates[10] of the size of the electron pockets on the basis of the Shubnikov–de Haas oscillations argued more in favor of a "direct" nesting vector $\mathbf{Q} = (2k_F, 0, 0)$. Measurements[5,6] of the Hall constant in $(TMTSF)_2ClO_4$ now permit us to assume with considerable assurance that the superstructure vector is direct and that the spectrum is of the form (1), (1′). This assurance is due, in particular, to the nontrivial experimental consequences which stem from the specific features of dispersion relation (1′) and which we shall now discuss.

To find the stability region of a metal with the dispersion relation (1), (1′), let us consider the generalized susceptibility of the system in the presence of a SDW (CDW) perturbation

$$\hat{\Delta}(x) = \begin{cases} \Delta(\hat{\sigma}_y)_{\alpha\beta} \exp(iQx), \\ \Delta \exp(i\ddot{Q}x), \end{cases} \quad (2)$$

($\hat{\sigma}$ is a Pauli matrix), where the vector $\mathbf{Q}$ is chosen in the form

$$\mathbf{Q} = (2k_F + k, 0, 0). \quad (3)$$

Here and below we assume, as usual, that the pressure increases the tunneling integral t_b, and so the metallic phase is realized for $P > P \equiv P(t_b^0)$. We shall see that all the results apply in equal measure (in the weak-field region and for the specified dispersion relation) to both SDW and CDW pairing. The majority of the formulas do not depend on the choice of order parameter in (2). Therefore, to avoid complicating the exposition by allowance for the spin variables, we shall drop them everywhere. In general terms we shall sometimes refer to the transition to the new phase as an excitonic transition.

The problem in the absence of magnetic field has been studied previously,[11] and we shall briefly list the features of the phase diagram which are peculiar only to dispersion relation (1) or (1′). For example, it turns out that in case (1′) at $T = 0$ stability considerations do not determine the periodicity of the superstructure at all—the stability of the metallic phase is insensitive to the choice of structure vector (3) for $|k| \leqslant 4t_b/v$. If, on the other hand, $t_c \neq 0$, the degeneracy is limited to the region $|k| \leqslant 4(t_b - t_c)/v$. The curve of the transition temperature $T(P)$ also behaves in an unusual manner. In the neighborhood $0 \leqslant P_0 - P \ll P_0$ this temperature has a nontrivial dependence on the pressure:

$$T = t_b^0 \left(\ln \frac{P_0}{P_0 - P} \right)^{-1}.$$

This kind of dependence is typical in the case of the formation of soliton superstructures. Finally, in the insulating phase ($k = 0$) the solution of the self-consistency equation for the gap is a step function:

$$\Delta = \begin{cases} \Delta_0, & t_b < \Delta_0/2, \\ 0, & t_b > \Delta_0/2. \end{cases}$$

For $t_b < \Delta_0/2$ the energy bands

$$\varepsilon_{1,2}(p_\parallel, \mathbf{p}_\perp) = 2t_b \cos(p_b b^*) \pm [(p_\parallel - k_F)^2 v^2 + \Delta_0^2]^{1/2}$$

do not overlap, and in this case, as usual,[12] Δ does not depend on t_b. Thus, the two-dimensional dispersion relation (1′) is characterized by the discontinuous vanishing of the gap at $t_b = t_b^0 = \Delta_0/2$ (there is no hysteresis!). If $t_c \neq 0$, "pockets" of carriers form with increasing t_b (as long as $t_b + t_c > \Delta_2 > t_b - t_c$), while for $\Delta = 2(t_b - t_c)$ the transition to the metallic phase occurs as before with the discontinuous vanishing of the gap Δ.

This behavior of the order parameter $\Delta(t_b)$ should be manifested experimentally in a substantial difference between the value of the optical gap of $(TMTSF)_2X$ compounds and the value of the activation energy $\Delta_a = 2\Delta - 4t_b$, which determines the low-temperature behavior of the static susceptibility.[2]

3. INSTABILITY OF A LAYERED QUASI-ONE-DIMENSIONAL METAL IN A MAGNETIC FIELD

Let us digress for a moment from the specific electronic spectrum of the Bechgaard salts to a more general type of spectrum:

$$\varepsilon_{1,2}(p_\parallel, \mathbf{p}_\perp) = \pm v(p_\parallel \mp k_F) + t(\mathbf{p}_\perp), \quad (4)$$

where the "Fermi momentum" k_F is determined by assigning the number of carriers:

$$\int d\mathbf{p}_\perp t(\mathbf{p}_\perp) = 0. \quad (4')$$

Let us study the features of the response of a system of noninteracting electrons, without specifying the type of perturbation (2) (diagram in Fig. 2):

$$\chi_0(k) = T \sum_{\omega_n} \int \frac{d\mathbf{p}_\perp}{S_\perp} \int dx' \exp[ik(x' - x)] g_{++}(i\omega_n, \mathbf{p}_\perp; x, x') \times g_{--}(i\omega_n, \mathbf{p}_\perp; x', x), \quad (5)$$

where $S_\perp$ is the area of the transverse cross section of the

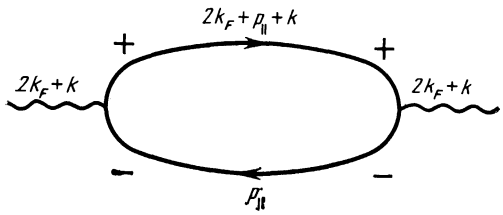

FIG. 2.

Brillouin zone. As usual, the magnetic field ($H \perp a$) with vector potential

$$\mathbf{A}=(0,\ Hx\cos\alpha,\ Hx\sin\alpha)$$

is taken into account by the replacement $p_\perp \to p_\perp - (e/c)A$. Then the slowly varying parts g_{++} and g_{--} of the right and left Green's functions

$$G_{\pm\pm}(i\omega_n,\ \mathbf{p}_\perp;\ x,\ x')=\exp[\pm ik(x-x')]\,g_{\pm\pm}(i\omega_n,\ \mathbf{p}_\perp;\ x,\ x')$$

satisfy the respective equations

$$\left\{i\omega_n \pm iv\frac{d}{dx}-t\left(p_b-\frac{eH\cos\alpha}{c}x,\ p_c-\frac{eH\sin\alpha}{c}x\right)\right\} \times g_{\pm\pm}(i\omega_n,\ \mathbf{p}_\perp;\ x,\ x')=\delta(x-x') \tag{6}$$

(for a CDW pairing, Eq. (6) really should include a term $\mu_B H$, but in what follows this term will always be negligible).

We now integrate (6) with allowance for the boundary conditions at infinity. We then have

$$g_{++}(i\omega_n,\ \mathbf{p}_\perp;\ x,\ x')=\frac{\operatorname{sign}\omega_n}{iv}\exp\left\{-\frac{\omega_n(x-x')}{v} -\frac{i}{v}\int_{x'}^{x}t\left(p_b-\frac{eHu\cos\alpha}{c},\ p_c-\frac{eHu\sin\alpha}{c}\right)du\right\} \tag{7}$$

for $\omega_n(x-x')/v>0$, and in the opposite case g_{++} is zero [for the function g_{--} the sign of the frequency in (7) should be changed]. Substituting (7) into (5), we finally get for the response of a system of noninteracting electrons

$$\chi_0(k)=\int\frac{d\mathbf{p}_\perp}{S_\perp}\int_0^\infty dx\,\frac{2\pi T}{v\sinh(2\pi Tx/v)} \times\left\{\exp\left[-\frac{i}{v}\int_0^x t\left(p_b-\frac{eHu\cos\alpha}{c},\ p_c-\frac{eHu\sin\alpha}{c}\right)du\right] \times\cos kx+\text{c.c.}\right\}, \tag{8}$$

where for small x the integral is cut off at atomic distances $d\sim\hbar v/E_F$.

We see that in the two-dimensional case the periodicity of the function in the exponential allows the vector k to be chosen commensurate with the period of this function, and integral (8) for $T=0$ diverges logarithmically at large distances. Actually, for layered compounds $t(\mathbf{p}_\perp)\equiv t(p_b)$, and therefore with allowance for the definition of the Fermi momentum (4') the inside integration over du gives a phase which depends periodically on the variable x. The integral (8) is cut off at large distances only by the temperature. In the general three-dimensional case this is of course not true, since the integration in (8) along an arbitrary straight line lying in the transverse cross section of the Brillouin zone does not necessarily lead to a periodic function in the exponential.

If χ_0 diverges logarithmically, then it is, as usual, necessary to take the interaction of the electrons into account. Summation of the series of ladder diagrams gives a criterion of the Stoner type for the stability of the metal:

$$\chi(k)=\chi_0(k)/[1-g\chi_0(k)],\qquad g\chi_0(k)\leqslant 1, \tag{9}$$

where $g>0$ is the effective electron-electron interaction constant. As in the Cooper effect, expression (9) with the appropriate sign of the interaction indicates the absolute instability of a two-dimensional metal with open Fermi surfaces in an arbitrarily weak magnetic field.

4. PHASE TRANSITION TEMPERATURE

Let us return, however, to the properties of the family of Bechgaard salts. The choice of a coupling constant in these compounds is determined by the type of transition in the absence of magnetic field at $P=0$. In view of the existing experiment, we shall henceforth discuss specifically SDW pairing. We choose the wave vector in form (3) and the electronic spectrum in form (1), (1'). The magnetic field is assumed parallel to the c^* axis.

Substituting (1) into (8), we write the stability criterion for the metallic state [i.e., a positive denominator in (9)] in the form

$$\Phi_0(k,\ T)+\Phi(\lambda,\ \mu,\ T)\geqslant 0, \tag{10}$$

in which we have separated out the magnetic-field dependence of the diagram in Fig. 2:

$$\Phi(\lambda,\mu,T)=-\int_0^\infty[J_0(2\lambda\sin\varphi)-J_0(2\lambda\varphi)]J_0\left(2\lambda\frac{t_c}{t_b}\varphi\right) \times\frac{\cos(2\mu\varphi)\,\pi T\lambda d\varphi}{t_b\sinh(\pi T\lambda\varphi/t_b)}, \tag{10'}$$

$$\Phi_0(k,T)=\frac{1}{g}-\int_0^\infty J_0\left(\frac{4t_b}{v}x\right)J_0\left(\frac{4t_c}{v}x\right) \times\cos(2kx)\,\frac{2\pi T dx}{v\sinh(2\pi Tx/v)} \tag{10''}$$

(we assume that it is the metallic state that is realized in the absence of the field, i.e., that $\Phi_0>0$). In (10') we have introduced the notation

$$\lambda=4t_b c/eHvb^*,\qquad \mu=\lambda kv/4t_b, \tag{11}$$

and $J_0(x)$ is the Bessel function of order zero.

For $T_b/t_c\gg 1$, expressions (10') and (10'') simplify:

$$\Phi(\lambda,\mu,T)=-\int_0^\infty[J_0(2\lambda\sin\varphi)-J_0(2\lambda\varphi)]\frac{\cos(2\mu\varphi)\,\pi T\lambda d\varphi}{t_b\sinh(\pi T\lambda\varphi/t_b)} \tag{12}$$

$$\Phi_0(k,T)=\frac{1}{g}-\int_0^\infty J_0\left(\frac{4t_b}{v}x\right)\cos(2kx)\frac{2\pi T dx}{v\sinh(2\pi Tx/v)} \quad (12')$$

(the role of the "three-dimensionality" of the electronic spectrum, $t_c \neq 0$, will be discussed separately).

The magnetic-field dependence $T(\lambda)$ of the temperature of the phase transition from the metal to the SDW state is included in the dependence of $\Phi(\lambda,\mu,T)$ on the dimensionless parameter λ. Since several parameters appear in (10), it is necessary to find the maximum value of T as a function (given implicitly for fixed λ) of the wave vector $k(\mu)$:

$$\Phi_0(k,\ T)+\Phi(\lambda,\ \mu,\ T)=0. \quad (12'')$$

Let us consider the weak-field case ($H\to 0$), where the parameter $\lambda\to\infty$. In this limit the problem simplifies substantially, since the transition temperature $T(\lambda)$ is exponentially small. Therefore, one can evaluate (12) keeping only the leading terms in $1/\lambda$, which give the required accuracy, and neglect all the corrections in powers of T.

In this region function (12') depends only weakly on the temperature (see Appendix 1) and is given by

$$\Phi_0(k,\ T)=\ln(t_b/t_b^0).$$

As to integral (12), let us first evaluate it to logarithmic accuracy by averaging the integrand in (12) over the rapidly oscillating Bessel function:

$$\Phi(\lambda,\ \mu T)\approx J_n^2(\lambda)\ln(T\lambda/t_b). \quad (13)$$

In deriving (13) we have used the formula

$$J_0(2\lambda\sin\varphi)=J_0^2(\lambda)+2\sum_{m=1}^{\infty}J_m^2(\lambda)\cos(2m\varphi).$$

Formula (13) thus determines $T(\lambda)$ for "commensurate" [see (11)] vectors

$$k=4t_b n/\lambda v. \quad (14)$$

Choosing from (13) the maximum value of $J_n^2(\lambda)$ for $|n|\approx\lambda$, we obtain the following magnetic-field dependence for the stability curve:

$$T(\lambda)=(t_b/\lambda)\exp[-2.2\lambda\ln(t_b/t_b^0)] \quad (15)$$

(here we have used the asymptotic form of $J_n(\lambda)$ for $\lambda-n\sim\lambda^{1/3}$).

Relation (13) explicitly contains the result of the previous section regarding the instability of a layered quasi-one-dimensional metal even in an arbitrarily weak magnetic field. In addition, it shows how that result is related to the degeneracy of the stability curve $T(k)$ for spectrum (1') at $H=0$: the same degeneracy is also present in (13) at small $n(k)$, since for $n\sim 1$ the asymptotic behavior of the Bessel function for $\lambda\gg 1$ does not depend strongly on the index n. The magnetic field, however, lifts the degeneracy in favor of larger $|k|\approx 4t_b/v$, since, as we have said, the function $J_n^2(\lambda)$ attains its maximum for $|n|\approx\lambda$. Consequently, the instability corresponds to the superposition of the parts of the Fermi surface with a wave vector $\mathbf{Q}$ from (3):

$$Q\approx 2k_F\pm 4t_b/v. \quad (16)$$

Such a superposition can be interpreted as the formation of rather large "pockets" of carriers (see Fig. 3) with an effective area of the "orbits"

$$S\approx 8\pi t_b/\hbar v b^*. \quad (17)$$

We emphasize again that this result stems from the choice of spectrum (1') and vector Q from (3) and, consequently, the experimental results, which indicate large pockets, apparently argue in favor of just such a situation.[5,6]

Let us study (13) in more detail. In the neighborhood $|\lambda-n|\sim\lambda^{1/3}$ the function $J_n^2(\lambda)$ changes little as a function of n. Equation (15) gives only the monotonic part of $T(\lambda)$. In deriving (13) we also used a discrete set of possible instability wave vectors (14). When H changes the index n changes, but we shall show presently that $T(\lambda)$ corresponds to integer μ. Small nonmonotonic oscillations thus arise against the background of the function $T(\lambda)$ from (13).

We have already seen that the important region is $\lambda-\mu\sim\lambda^{1/3}$. In the integral (12), by excluding for the time being the immediate neighborhood of $\varphi=0$, we can neglect the term $J_0(2\lambda\varphi)$. The remaining product of rapidly oscillating Bessel functions and $\cos(2\mu\varphi)$ gives the main contribution to the integral near the points $\varphi=\pi m$. By neglecting the slow dependence of the temperature factor, we can easily express the contribution in the neighborhoods of these points in terms of the square of the Bessel function [or, more precisely, its asymptotic behavior for $\lambda-n\sim\lambda^{1/3}$ (see Appendix 2)]. We denote this contribution by $\Phi_2(\lambda,\mu)$. After this, and with allowance for the neighborhood of $\varphi=0$ [the contribution from which we denote $\Phi_1(\lambda,\mu)$], integral (12) can be rewritten in the form of a series

$$\Phi(\lambda,\mu,T)=\Phi_1(\lambda,\mu)-\Phi_2(\lambda,\mu)\sum_{m=1}^{\infty}\frac{\pi^2 T\lambda\cos(2\mu\pi m)}{t_b\sinh(\pi^2 T\lambda m/t_b)}. \quad (18)$$

We recall that $\Phi(\lambda,\mu,T)$ is the contribution to the susceptibility which appears in the denominator of the Stoner crite-

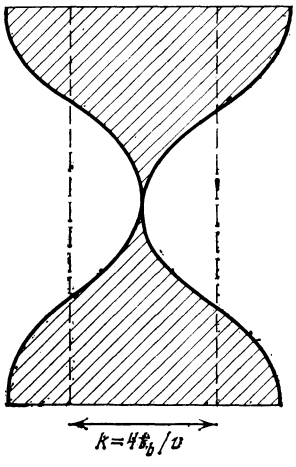

FIG. 3.

rion (9). Here $\Phi_2(\lambda,\mu)>0$, and we see that the minimum values of the sum in (18) actually are reached at integral values of μ [otherwise there is no logarithmic divergence for $T\to 0$ in (18)]. We are now interested in the function $\Phi_2(\lambda,\mu)$ itself in the region of the maximum ($|\mu-\mu^*(\lambda)|\ll\lambda^{1/3}$), where it is of the form

$$\Phi_2(\lambda,\ \mu)\approx 0.46\lambda^{-2/3}-0.74\lambda^{-4/3}[\mu-\mu^*(\lambda)]^2,$$
$$\mu^*(\lambda)\approx\lambda-0.81\lambda^{1/3} \qquad (19)$$

(see Appendix 2). Thus μ must be an integer, the one closest to $\mu^*(\lambda)$. As λ changes, according to (19) and the definition of $\mu^*(\lambda)$, there are jumps in the vector k (i.e., μ) with a period

$$\Delta(\lambda)=1. \qquad (20)$$

In this derivation we have used for the oscillations only the second term in (18), which we can do when the temperatures are exponentially small [the sum in (18) is replaced by a logarithmic integral]. We assume that the system is found at the stability threshold: $t_b-t_b^0\ll t_b^0$. Then, in fields $\lambda^{1/3}\ll t_b/(t_b-t_b^0)$ the properties of $\Phi_1(\lambda,\mu)$ become important. As we show below, oscillations (20) still remain in this case.

It follows from (13) and (20) that the oscillations are small:

$$\Delta T(\lambda)/T(\lambda)\approx 0.88\ln(t_b/t_b^0)\ll 1. \qquad (21)$$

The fact that μ is close to $\mu^*(\lambda)$ also gives a smooth change in the vector k with field:

$$k=(4t_b/v)(1-0.81\lambda^{-2/3}). \qquad (22)$$

As to oscillations (20) and (21), the periodicity in the inverse field in (20) can be written

$$\Delta(1/H)=2\pi e\hbar/cS, \qquad (20')$$

where S is given by (17). Figure 4 shows the results of a numerical solution of equation (12″) for $0<\lambda<5$, where the law (20) can be clearly discerned.

Finally, let us give the form of the function $\Phi_1(\lambda,\mu)$ for $\mu\approx\mu^*(\lambda)$:

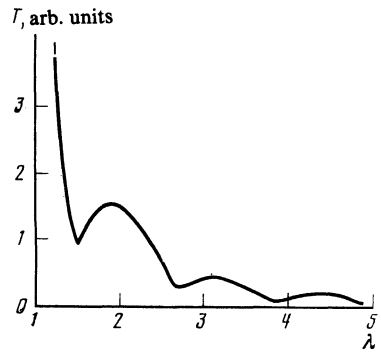

FIG. 4.

$$\Phi_1(\lambda,\ \mu)\approx 0.20\lambda^{-1/3}+0.25\lambda^{-2/3}[\mu-\mu^*(\lambda)]. \qquad (23)$$

The first term is important for determining the monotonic dependence of the instability temperature, while the functional dependence of $\Phi_1(\lambda,\mu)$ on μ must be taken into account at higher temperatures $T\sim t_b/\lambda$.

Let us consider the series (18) in this temperature region [as will become clear, this region is possible near the threshold, i.e., $(t_b-t_b^0)/t_b^0\ll 1$]. Then expression (18) as before has local minima at integer μ, but the global minimum of (18) is now determined by $\Phi_1(\lambda,\mu)$. After taking the asymptotic form of the formulas of Appendix 2, we can write series (18) in the neighborhood of the minimum of $\Phi_1(\lambda,\mu)$ in the form [not to be confused with expansion (23)]:

$$\Phi(\lambda,\mu,T)\approx-\frac{0.22}{\lambda^{1/3}}+\frac{1.00[\mu-\tilde{\mu}(\lambda)]^2}{\lambda}$$
$$-\frac{0.44}{\lambda^{2/3}}\sum_{m=1}^{\infty}\frac{\pi^2T\lambda\cos(2\mu\pi m)}{t_b\sinh(\pi^2T\lambda m/t_b)}, \qquad (24)$$

where $\mu(\lambda)\approx\lambda-0.93\lambda^{1/3}$. We see from (24) that oscillations (20) remain, but their detailed analysis requires numerical calculations.

Thus, the stability curve in the purely two-dimensional case is characterized by rapid oscillations [(20), (21)] superposed on a rapid increase of $T(\lambda)$ with increasing field. Having expansion (18), we can obtain, in place of (15), an expression for $T(\lambda)$ accurate to within corrections to the coefficient of the exponential:

$$T(\lambda)=\frac{2\gamma t_b}{\pi^2\lambda}\exp\left[-2{,}2\lambda^{2/3}\ln\frac{t_b}{t_b^0}-0{,}4\lambda^{1/3}\right],$$

where γ is the Euler constant.

5. STABILITY CURVE OF A QUASI-ONE-DIMENSIONAL CONDUCTOR

In this brief section we discuss how t_c (1)—the "three-dimensionality" of the electronic spectrum—affects the stability curve of a quasi-one-dimensional conductor in a field. The fact that a threshold field arises for finite t_c follows from (10′). If t_c is small, or, more precisely, if $t_c\sim T$ in the approximation of Sec. 4, an estimate for the threshold field is obtained from (15) by the replacement $T\to t_c$. However, we see from (10′) that the cutoff due to the second Bessel function occurs at $\varphi\sim t_b/\lambda t_c$. For realistic values of the parameter this cutoff causes the logarithmic contribution to the integral to vanish. In the general case $T\sim t_c$ one can study (10) only by numerical methods. For $T\gg t_c$ the results of the previous section are approximately correct. Therefore, let us now consider the opposite case, $T\ll t_c$, and let $1\ll\lambda t_c/t_b\ll\lambda^{1/3}$. We study (10′) and (10″) in the region $\lambda-\mu\sim\lambda^{1/3}$, which is the only important region in what follows. From a mathematical standpoint the difference from Sec. 4 lies only in a change in the form of the terms in sum (18) which correspond to the integration in (10′) in each of the small neighborhoods of the integer values $\varphi/\pi=m$. The corresponding sum assumes the form [cf. (18)]:

$$\Phi(\lambda,\mu,T)=\Phi_1(\lambda,\mu,T)-\Phi_2(\lambda,\mu)\frac{1}{2\pi^2}\left(\frac{t_b}{\lambda t_c}\right)^{1/2}$$

$$\times\sum_{m=1}^{\infty}\frac{1}{m^{3/2}}\left\{\cos\left(2\lambda\frac{t_c}{t_b}\pi m+2\mu\pi m-\frac{\pi}{4}\right)\right.$$

$$\left.+\cos\left(2\lambda\frac{t_c}{t_b}\pi m-2\mu\pi m-\frac{\pi}{4}\right)\right\}, \tag{25}$$

and it is necessary to keep the temperature dependence of the function $\Phi_1(\lambda,\mu,T)$:

$$\Phi_1(\lambda,\mu,T)=\Phi_1(\lambda,\mu)+\frac{\pi^2T^2\lambda}{24t_b^2}\frac{\partial^2\Phi_1(\lambda,\mu)}{\partial\mu^2}.$$

In deriving (25) we have made use of the fact that in integral (10′) near zero ($\varphi\sim\lambda^{-1/3}$) one can set

$$J_0\left(2\lambda\frac{t_c}{t_b}\varphi\right)\approx 1,$$

while for $\varphi\approx\pi m$ it is sufficient to use the asymptotic expression

$$J_0\left(2\lambda\frac{t_c}{t_b}\varphi\right)\approx\left(\frac{t_b}{2\lambda t_c\pi\varphi}\right)^{1/2}\cos\left(2\lambda\frac{t_c}{t_b}\varphi-\frac{\pi}{4}\right). \tag{25′}$$

The series in (25) is a small correction to $\Phi_1(\lambda,\mu,T)$. Analysis of this series shows that $\Phi(\lambda,\mu,T)$ on the whole has local minima at integer values $\mu\pm\lambda t_c/t_b$. We assume, for example, that $\mu+\lambda t_c/t_b=N$, where N is an integer. In contrast to the situation in Sec. 4, we can now neglect the change by unity of the integer parameter $\mu+\lambda t_c/t_b$. Therefore, in the neighborhood of the minimum of the function $\Phi_1(\lambda,\mu)$, we rewrite (25) in the form (see Appendix 2)

$$\Phi(\lambda,\mu,T)\approx-\frac{0{,}22}{\lambda^{1/3}}+\frac{0{,}82}{\lambda}\left(\frac{T\lambda}{t_b}\right)^2-\frac{0{,}04}{\lambda^{2/3}}\left(\frac{t_b}{\lambda t_c}\right)^{1/2}$$

$$\times\sum_{m=1}^{\infty}\frac{1}{m^{3/2}}\left[\frac{1}{\sqrt{2}}+\cos\left(4\lambda\frac{t_c}{t_b}\pi m-\frac{\pi}{4}\right)\right]. \tag{26}$$

Taking in (26) the leading term (for $T=0$), we obtain for the critical field H_0

$$H_0\approx\frac{400t_bc}{evb^*}\left(\ln\frac{t_b}{t_b^0}\right)^3, \tag{26′}$$

while the temperature dependence of the critical field is

$$H(T)=H_0[1+11\lambda_0^{4/3}(T/t_b)^2], \tag{26″}$$

where λ_0 and H_0 are related by (11).

Allowance for the terms in series (26) which are periodic [with period $\Delta(\lambda)=t_b/2t_c$] in the parameter λ gives rise to slow [in comparison with (20)], small-amplitude oscillations of the critical field and transition temperature, with a period in the inverse field of

$$\Delta(1/H)=(2\pi e\hbar/cS)(t_b/2t_c) \tag{27}$$

[recall that S is given by (17)].

The physical meaning of the oscillations (27) is as follows. For $t_c\neq 0$ the main contribution to the nonmonotonic part of the generalized susceptibility is from those electrons on the Fermi surface for which the velocity along the c^* axis is zero (they do not separate to infinity). These electrons, with $p_c=0$ and $p_c=\pi/c^*$, give two sets of optimum vectors [cf. (14)]:

$$k_1=t_c+4t_bn_1/v\lambda,\qquad k_2=-t_c+4t_bn_2/v\lambda. \tag{28}$$

For integer values of the combination $2\lambda t_ct_b$, expressions (28) become the same, which causes the susceptibility contributions from electrons with $p_c=0$ and $p_c=\pi/c^*$ to be summed and, consequently, enhances the insulator pairing.

6. EXCITONIC SUBPHASES

It was shown above that the phase transition temperature of a layered quasi-one-dimensional metal in a SDW state oscillates rapidly in a magnetic field and that its dependence on H consists essentially of two separate pieces, corresponding to different wave vectors $k(n)$. Therefore, at temperatures below the stability curve the system undergoes transitions to successive excitonic subphases as the magnetic field increases.

Let us consider the general term of the free-energy expansion of a conductor with dispersion relation (1′) in powers of the order parameter $\tilde{\Delta}(x)=\exp(i2k_Fx)\Delta(x)$. Obviously, an arbitrary term of the variation of the free energy is of the form

$$\frac{\delta F_m}{\delta\Delta(x)}=-T\sum_{\omega_n}\int dx_1\ldots\int dx_{2m+1}\int\frac{dp_bb^*}{2\pi}g_{++}(i\omega_n,p_b;x,x_1)$$

$$\times\Delta(x_1)\ldots\Delta(x_{2m+1})g_{--}(i\omega_n,p_b;x_{2m+1},x), \tag{29}$$

where $\Delta(x)=\Delta\exp(ikx)$. After substitution of (7) into (29) it is convenient to introduce the new variables

$$\alpha_k=\begin{cases}x-x_1, & k=0\\ x_{2k}-x_{2k+1}, & 1\leqslant k\leqslant m,\end{cases}$$

$$\beta_k=\tfrac{1}{2}(x+x_1-x_{2k}-x_{2k+1}),\quad 1\leqslant k\leqslant m,$$

and to shift the integration over p_b:

$$p_b\to p_b-\tfrac{1}{2}(e/c)H(x_1+x).$$

As a result we obtain

$$\frac{dF_m}{d\Delta}=2\Delta^{2m+1}\sum_{\omega_n>0}\int_0^\infty d\alpha_0\ldots\int_0^\infty d\alpha_m\int d\beta_1\ldots\int d\beta_m$$

$$\times\exp\left[-\frac{(2\omega_n+i\Delta k)(\alpha_0+\ldots+\alpha_m)}{\hbar v}\right]\Pi_n(\lambda), \tag{30}$$

where

$$\Pi_n(\lambda)=\exp[-ik(n)(\alpha_0+\ldots+\alpha_m)]\int\frac{dp_bb^*}{2\pi}$$

$$\times\exp\left\{-2i\lambda\left[\sin\left(\frac{2t_b\alpha_0}{v\lambda}\right)\cos(p_bb^*)+\ldots\right.\right.$$

$$\left.\left.+\sin\frac{2t_b\alpha_m}{v\lambda}\cos\left(p_bb^*+\frac{2t_b}{v\lambda}\beta_m\right)\right]\right\}, \tag{30′}$$

while the integration over the variables β is limited to the region

$$\alpha_k+\beta_k+\alpha_{k+1}>\beta_{k+1}, \quad \alpha_0+\alpha_1-\beta_1>0,$$

$$\alpha_0+\alpha_m+\beta_m>0, \quad 1\leqslant k\leqslant m-1$$

[here $k(n)$ is one of the wave vectors (14), and $\Delta k = k - k(n)$].

In a weak magnetic field ($\lambda\to\infty$) the excitonic subphases in the two-dimensional case exist in a region of exponentially low temperatures $T\leqslant T(\lambda)$. Therefore, for $\Delta k \ll v\lambda/t_b$ the integrand in (30′) can be averaged over the rapid oscillations, since the integral in (30) converges with respect to all variables at large distances of the order of $\min(v/T, v/\Delta k)$. As a result we obtain

$$\overline{\Pi}_n(\lambda) = J_n^{2(m+1)}(\lambda) \tag{31}$$

[here the overbar denotes an average, and the index n of the Bessel function is, as before, related to the wave vector by (14)]. After (31) has been obtained, the sum and the integrals appearing in (30) are transformed to the corresponding expansions of the variation of the free energy for an effective Peierls-transition problem.

In other words, an arbitrary term of the free-energy expansion of a layered quasi-one-dimensional conductor with spectrum (1′) in the presence of a magnetic field can be obtained from the expression for the Peierls free energy by the replacement $\Delta^2\to\Delta^2 J_n^2(\lambda)$. The terms of second order in Δ are an exception. They, however, have already been evaluated in Sec. 4 and correspond to an "effective coupling constant"

$$1/g\to[\ln(t_b/t_b^0)+0.2\lambda^{-1/3}]/J_n^2(\lambda),$$

and a magnetic-field dependent cutoff constant $E^* = 2\gamma t_b/\pi^2\lambda$.

In this form the free energy in a magnetic field has local minima at $\Delta k = \Delta\mu = 0$, and for a subphase with wave vector $k(n)$ from (14) the entire sum of diagrams (30) is transformed into the functional

$$F(\lambda, n) = \Delta^2\left[\ln\frac{t_b}{t_b^0}+\frac{0.2}{\lambda^{1/3}}\right] - 4T\int_0^{E^*} d\xi \ln\left[\frac{\cosh([\xi^2+J_n^2(\lambda)\Delta^2]^{1/2}/2T)}{\cosh(\xi/2T)}\right], \tag{32}$$

where F is measured from the energy of the metallic state.

From here we must determine the phase diagram of the layered conductor. The free energy (32), of course, cannot be written in closed form, but several conclusions can be drawn on the basis of its form. The condition that the variation of (32) with respect to Δ vanish determines the equilibrium value on the gap $\Delta_n(\lambda)$ for the $n-th$ subphase:

$$\frac{-\ln(t_b^0/t_b)+0.2\lambda^{-1/3}}{J_n^2(\lambda)} - \int_0^{E^*} d\xi[\xi^2+\Delta_n^2(\lambda)J_n^2(\lambda)]^{-1/2}\tanh\frac{[\xi^2+\Delta_n^2(\lambda)J_n^2(\lambda)]^{1/2}}{2T} = 0. \tag{33}$$

With allowance for (33) we have

$$F(\lambda, n) = \int_0^{\infty} d\xi\left[\frac{J_n^2(\lambda)\Delta_n^2(\lambda)}{[\xi^2+J_n^2(\lambda)\Delta_n^2(\lambda)]^{1/2}}\tanh\frac{[\xi^2+J_n^2(\lambda)\Delta_n^2(\lambda)]^{1/2}}{2T} - 4T\ln\frac{\cosh([\xi^2+J_n^2(\lambda)\Delta_n^2(\lambda)]^{1/2}/2T)}{\cosh(\xi/2T)}\right] \tag{34}$$

[in the convergent integral (34) the upper limit has been set to infinity]. Since energy (34) of each subphase now depends explicitly only on $\tilde{\Delta}_n^2 = J_n^2(\lambda)\Delta_n^2(\lambda)$, it follows from (33) that the optimum values of $\tilde{\Delta}_n$ and wave vector $k(n)$ are reached at the maximum of $J_n^2(\lambda)$.

Thus, the phase diagram of a layered quasi-one-dimensional conductor at a temperature $T\leqslant T(\lambda)$ consists of subphases determined by the wave vectors k from (14) for which $J_n^2(\lambda)$ is maximum. According to Sec. 4, the vector of the SDW structure in this case is given approximately by $k\approx 4t_b/v$. A change in field produces small but sharp jumps in this vector, with a period in the inverse field given by (20). Simultaneously, oscillations develop in the insulator gap and other physical quantities in the two-dimensional model. In approximation (33)–(34) the phase transition from the metal to the SDW state and the transitions between subphases (the jumps of the wave vector) correspond to second order transitions. This last statement, however, is only approximate—allowance for correction (23) leads to small jumps in the order parameter at the transition from subphase n to subphase $n+1$:

$$|\Delta_{n+1}(\lambda)-\Delta_n(\lambda)|/\Delta_n(\lambda)\sim\lambda^{-2/3}\ln(t_b/t_b^0). \tag{35}$$

The phase diagram of a layered conductor with dispersion relation (1′) is shown schematically in Fig. 5 (the broken vertical lines show the boundaries between excitonic subphases).

The phase diagram of a quasi-one-dimensional conductor with finite t_c cannot be found. In the region of parameters $\lambda t_c/t_b\sim 1$, after averaging the rapidly oscillating terms in the free-energy expansion in Δ one is left with sums over discrete variables in place of the corresponding integrals

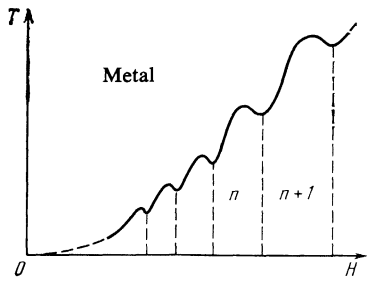

FIG. 5.

(see Sec. 5), which cannot be represented in analytical form. Therefore, for $t_c \neq 0$ we must confine ourselves to a study of the stability curve.

7. CONCLUSION

Let us compare our results with what can be inferred from experiment. It is known[13] that, at least in the weak-field region $H \approx H_0$, the transition from the metallic to the excitonic phase is second order. Thus it is sensible to calculate the stability curve. In addition, at low temperatures the transitions from one subphase to another have been found to exhibit a small hysteresis, the size of which at the position of the "Shubnikov–de Haas oscillations" increases with the field but falls off with temperature.[14] The possibility of a small hysteresis at low temperatures is indicated by the result (35). It is clear that three-dimensional effects will alter this result, apparently with the effect of increasing the hysteresis and lengthening the period [see (27)], but we have no way to give a rigorous quantitative description of this. However, accepting as an experimental fact that the hysteresis falls off with increasing temperature, we attribute the rapid oscillations observed[6] in the region of large H and T to oscillations (20′) (here $T \sim t_c$). Introducing $v = t_a a\sqrt{2}\hbar$ (where t_a is the tunneling integral along the chain), we find from (20′) that $t_a/t_b \approx 24$, in fair correspondence with Ref. 1. Substituting this value into the definition of λ (11), we get

$$\lambda = 275/H[\mathrm{T}].$$

Passing now to the low-temperature region, where significantly, $t_c > T$, and taking the data[5,6] from the corresponding "Shubnikov–de Haas oscillations," we find from (27) that $t_b/t_c \approx 22$. Estimates based on the conductivity[1] usually give $t_b/t_c \approx 10$–30 (i.e., $t_c \approx 10$ K).

Expression (26′) for the critical field H_0 for the appearance of the magnetic phase requires special discussion here. The experimental[5,6] values $H_0 \approx 4$–5 T can be obtained by assuming that all the effects develop at the (pressure) threshold for the existence of the metallic phase, $(t_b - t_b^0)/t_b^0 \approx 0.06$. Taking $H_0(T)$ from Ref. 5 and using (26″) in the case $X = ClO_4$, we have $t_b \approx 150$ K, which is close to the experimental data.[1] As long as we see that the situation appears reasonable, it makes sense to give the asymptotic expression for $T(\lambda)$ in the region where $1 \ll T\lambda/t_b \ll \lambda^{1/3}$, which can easily be obtained from (12) by expanding in φ about zero:

$$T = 0.3\,\frac{t_b}{\lambda^{2/3}}\left(\frac{H-H_0}{H}\right)^{1/2}$$

($\mu \approx \lambda$). This temperature region has not been attained experimentally.[14]

Hall-effect experiments indicate that at low temperatures the subphases formed have a semimetallic character with rather large carrier pockets. Although the transitions between subphases and the band structure in the subphases remain outside our treatment (since here $t_c > T$), the order of magnitude of the pockets in the first subphases is estimated according to (17) and Fig. 3 as $n \sim 10^{20}$ cm^{-3}, which again agrees with experiment and stands, I believe, as the main argument in favor of the choice of a direct nesting vector (3).

Attempts have been made[15,16] to construct the excitonic phases in a magnetic field under the assumption that the stability of the insulating phase is increased on account of the overall lowering of the energy in the band gap because of the quantization of the levels. The oscillation effect was attributed to the filling of the successive Landau levels with increasing field.[16] It seems to me that the change of the energy of the excitonic phase in a field requires a more correct calculation of the electronic density of states in the presence of a field than was given in Ref. 15. Furthermore, this picture recognizes the vital importance, even in weak magnetic fields, of the change in the superstructure vector (3) in comparison with the nesting vector in the absence of field.

I am deeply grateful to L. P. Gor'kov for directing this study and to L. N. Shchur for much help in the numerical calculations.

APPENDIX 1

In function (10″) we separate out the contribution to the integral for $k = t_b = t_c = 0$:

$$\Phi_0(k,T) = \ln\frac{T}{T_0} + \int_0^\infty \Big[\, 1 - \cos\Big(\frac{4t_b x}{v}\sin\varphi_1\Big) \times \cos\Big(\frac{4t_c x}{v}\sin\varphi_2\Big)\cos(2kx)\,\Big]_{1,2} \frac{2\pi T\,dx}{v\sinh(2\pi T x/v)}. \tag{A1.1}$$

Here we have used the representation of the Bessel function

$$J_0(z) = \frac{1}{\pi}\int_0^\pi \cos(z\sin\varphi)\,d\varphi$$

and denoted by subscripts 1 and 2 the averaging over φ_1 and φ_2, respectively. Integral (A1.1) is conveniently rewritten in the form of a series[17]:

$$\Phi_0(k,T) = \ln\frac{T}{T_0} + \sum_{n=0}^{\infty}\Big\{\frac{1}{2n+1} - \Big[\,4n+2+\frac{4i}{\pi T}\Big(t_b\cos\varphi_1 + t_c\cos\varphi_2 + \frac{kv}{4}\Big)\Big]^{-1} - \Big[\,4n+2+\frac{4i}{\pi T}\Big(t_b\cos\varphi_1 + t_c\cos\varphi_2 - \frac{kv}{4}\Big)\Big]^{-1}\Big\}_{1,2}$$

and this series is replaced, in turn, by a contour integral in the complex plane:

$$\Phi_0(k,T) = \ln\frac{T}{T_0} + \int_{-\infty}^{\infty}\mathrm{th}\frac{z}{2T}\Big\{\frac{2}{z} - \Big[\,z^2 - 4\Big(t_b\cos\varphi_1 + t_c\cos\varphi_2 + \frac{kv}{4}\Big)^2\Big]^{-1} - \Big[\,z^2 - 4\Big(t_b\cos\varphi_1 + t_c\cos\varphi_2 - \frac{kv}{4}\Big)^2\Big]^{-1}\Big\}_{1,2}. \tag{A1.2}$$

Integrating by parts, we get

$$\Phi_0(k,T)=\ln\frac{t_b}{t_b^0}+\frac{1}{4}\int_0^\infty\Big[\ln\Big|\Big(\frac{z}{t_b}\Big)^2-\Big(2\cos\varphi_1+2\frac{t_c}{t_b}\cos\varphi_2+\frac{kv}{2}\Big)^2\Big|+\ln\Big|\Big(\frac{z}{t_b}\Big)^2-\Big(2\cos\varphi_1+2\frac{t_c}{t_b}\cos\varphi_2-\frac{kv}{2}\Big)^2\Big|\Big]_{1,2}\times\frac{dz}{2\pi T\cosh^2(z/2\pi T)},\qquad\text{(A1.3)}$$

where $t_b^0=\pi T_0/2\gamma$.

It is a property of (A1.3) that the integral over the variable φ_1 is nonzero only for $z>2(t_b-t_c)-kv/2$. Therefore, in the parameter region $\lambda-\mu\sim\lambda^{1/3}$, $\lambda t_c/t_b\ll\lambda^{1/3}$ the function $\Phi_0(k,T)$ does not depend on the variables k and T to exponential accuracy in the parameter $t_b/T\lambda^{2/3}$.

APPENDIX 2

We write the contribution from the integration of (12) in the neighborhood of $\varphi=0$ as

$$\Phi_1(\lambda,\mu)=-\frac{1}{2(\pi\lambda)^{1/2}}\int_0^\infty\frac{d\varphi}{\varphi^{3/2}}\Big\{\cos\Big[2(\mu-\lambda)\varphi+\lambda\frac{\varphi^3}{3}+\frac{\pi}{4}\Big]-\cos\Big[2(\mu-\lambda)\varphi+\frac{\pi}{4}\Big]\Big\}.\qquad\text{(A2.1)}$$

In going from (12) to (A2.1) we have used asymptotic expression (25′) and kept the leading terms. Integrating (A2.1) by parts, we obtain the differential equation

$$\Phi_1(\lambda,\mu)=2(\mu-\lambda)\Phi_1'-{}^1/_4\lambda\Phi_1''',\qquad\text{(A2.2)}$$

where the primes denote differentiation with respect to μ. It is convenient to differentiate (A2.2) with respect to μ and consider the equation for the derivative $y=\Phi_1'$:

$$y+2(\mu-\lambda)y'-{}^1/_4\lambda y'''=0,\qquad\text{(A2.3)}$$

which, as we know,[18] has a general solution of the form

$$y=c_1u^2+c_2uv+c_3v^2,\qquad\text{(A2.4)}$$

where $u(x)$ and $v(x)$ are linearly independent solutions of the Euler equation

$$u''-xu=0,\quad x=2^{1/3}(\mu-\lambda)/\lambda^{1/3}.\qquad\text{(A2.5)}$$

The values of the function $\Phi_1(\lambda,\mu)$ and its derivatives Φ', Φ'', and Φ''' at the point $\mu-\lambda=-0$ can be found immediately[17]:

$$\Phi_1'(-0)=\frac{2^{2/3}\pi}{3^{5/6}\Gamma^2(2/3)\lambda^{2/3}},\quad\Phi_1''(-0)=0,\quad\Phi_1'''(-0)=-\frac{2\cdot3^{1/3}\Gamma(5/6)}{\pi^{1/2}\lambda^{4/3}}$$

and it is therefore easy to choose from (A2.4) the necessary particular solution

$$y=2^{2/3}uv\lambda^{-2/3}.$$

With allowance for (A2.2) and (A2.5) we find

$$\Phi_1(\lambda,\mu)=\frac{2^{1/6}}{\lambda^{2/3}}\Big[u(x)v(x)-\frac{du}{dx}\frac{dv}{dx}\Big],$$

where $u(x)$ and $v(x)$ are determined by the standard boundary conditions:

$$u(0)=\pi^{1/2}3^{1/6}\Gamma(2/3),\quad v(0)=\pi^{1/2}3^{2/3}\Gamma(2/3),$$
$$u'(0)=3^{1/6}\pi^{1/2}/\Gamma(1/3),\quad v'(0)=\pi^{1/2}/3^{2/3}\Gamma(2/3).$$

Let us now consider the function $\Phi_2(\lambda,\mu)$, the contribution from the integration of (12) in the neighborhood of the points $\varphi=\pi m$ (m is a natural number):

$$\Phi_2(\lambda,\mu)=-\frac{1}{2(\pi\lambda)^{1/2}}\int_0^\infty\frac{d\varphi}{\varphi^{1/2}}\cos\Big[2(\mu-\lambda)\varphi+\lambda\frac{\varphi^3}{3}+\frac{\pi}{4}\Big].\qquad\text{(A2.6)}$$

Integrating (A2.6) by parts, we get for $\Phi_2(\lambda,\mu)$ the same differential equation (A2.3) but with a different boundary condition:

$$\Phi_2(-0)=\pi/2^{1/3}3^{4/3}\Gamma^2(2/3)\lambda^{2/3},\quad\Phi_2'(-0)=2^{2/3}\pi/3^{4/3}\Gamma^2(2/3)\lambda^{2/3}.$$

As a result, we have

$$\Phi_2(\lambda,\mu)=v^2(x)/2^{1/3}\lambda^{2/3}.$$

Let us also find the temperature dependence of $\Phi_2(\lambda,\mu,T)$. For this we expand $\sinh(\pi T\lambda\varphi/t_b)$ in (12) in powers of the small parameter $\lambda T\varphi/t_b$ up to and including the cubic term. The resulting integrals as before converge in a small neighborhood $\varphi\sim\lambda^{-1/3}$; therefore, we easily convince ourselves that

$$\Phi_1(\lambda,\mu,T)=\Phi_1(\lambda,\mu)+\frac{\pi^2T^2\lambda^2}{24t_b^2}\frac{\partial^2}{\partial\mu^2}\Phi_1(\lambda,\mu).$$

The mathematical tables of Ref. 19 are useful for finding the values of the functions $\Phi_1(\lambda,\mu)$ and $\Phi_2(\lambda,\mu)$ and their derivatives.

[1]D. Jerome and H. J. Schulz, Adv. Phys. **31**, 299 (1982).
[2]L. P. Gor'kov, Usp. Fiz. Nauk **144**, 381 (1984) [Sov. Phys. Usp. **27**, 809 (1984)].
[3]J. F. Kwak, J. E. Schirber, R. L. Green, and E. M. Engler, Phys. Rev. Lett. **46**, 1296 (1981).
[4]K. Kajimura, H. Tokumoto, M. Tokumoto, *et al.*, J. Phys. (Paris) Colloq. **C3**, 1059 (1983).
[5]M. Ribault, D. Jerome, J. Tuchendler, *et al.*, J. Phys. (Paris) Lett. **44**, L-953 (1983).
[6]P. M. Chaikin, Mu-Yong Choi, J. F. Kwak, *et al.*, Phys. Rev. Lett. **51**, 2333 (1983).
[7]L. P. Gor'kov and A. G. Lebed', J. Phys. (Paris) Lett. **45**, L-433 (1984).
[8]B. Horovitz, H. Gutfreund, and M. Weger, Phys. Rev. B **12**, 3174 (1975).
[9]L. V. Keldysh and Yu. V. Kopaev, Fiz. Tverd. Tela (Leningrad) **6**, 2791 (1964) [Sov. Phys. Solid State **6**, 2219 (1965)].
[10]J. F. Kwak, Phys. Rev. B **28**, 3277 (1983).
[11]S. A. Brazovskiĭ, L. P. Gor'kov, and A. G. Lebed', Zh. Eksp. Teor. Fiz. **83**, 1198 (1982) [Sov. Phys. JETP **56**, 683 (1982)].
[12]L. P. Gor'kov and T. T. Mnatsakanov, Zh. Eksp. Teor. Fiz. **63**, 684 (1972) [Sov. Phys. JETP **36**, 361 (1973)].

[13]R. Brusetti, P. Garoche, and K. Bechgaard, J. Phys. (Paris) Colloq. **C3**, 1051 (1983).
[14]R. L. Green and P. M. Chaikin, Physica B **126**, 431 (1984).
[15]K. Yamaji, Int. Conf. on the Phys. and Chem. of Low Dimensional Synthetic Metals, Abano Terme, Italy (1984).
[16]M. Heritier, G. Montambaux, and P. Lederer, J. Phys. (Paris) Lett. **45**, L-943 (1984).
[17]I. S. Gradshteĭn and I. M. Ryzhik, Tablitsy Integralov, Summ, Ryadov, i Proizvedeniĭ, Fizmatgiz, Moscow (1962) [Table of Integrals, Series, and Products, Academic Press, New York (1965)].
[18]E. Kamke, Differentialgleichungen, Lösungsmethoden und Lösungen, Bd. 1, Gewöhnliche Differentialgleichungen [in German], Akademische Verlagsgesellschaft, Leipzig (1942); reprinted Chelsea, New York (1971)].
[19]G. D. Yakovleva, Tablitsy Funktsiĭ Éĭri i Ikh Proizvodnykh [Tables of Airy Functions and Their Derivatives], Nauka, Moscow (1965).

Translated by Steve Torstveit